CENTER FOR CONNECTED AND AUTOMATED TRANSPORTATION

Final Report #70
August 2023

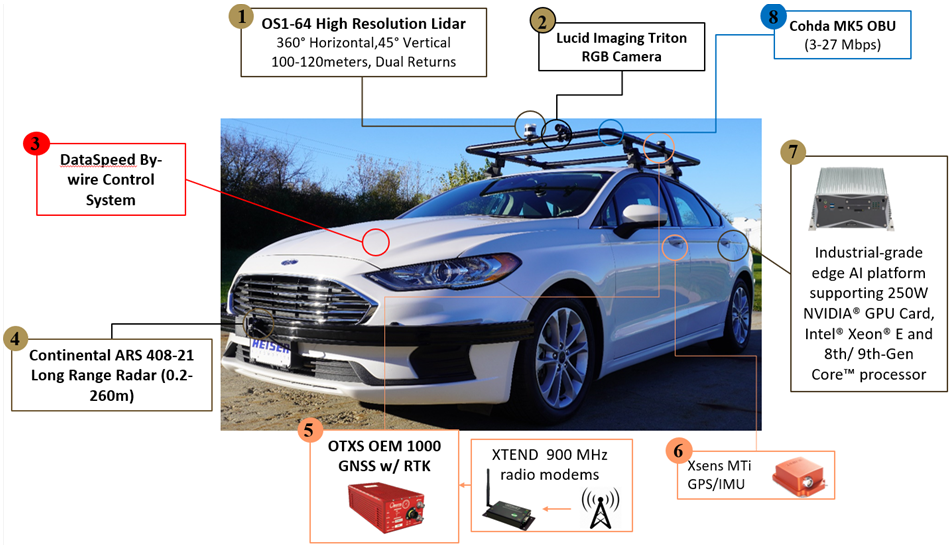

Development of a Cooperative Perception System

Yiheng Feng
Andrew Tarko

PURDUE UNIVERSITY®

CENTER FOR CONNECTED AND AUTOMATED TRANSPORTATION

Report No. CCAT Report No. 70
Report Date: August 2023
Project Start Date: April 2022
Project End Date: August 2023

Development of a Cooperative Perception System

By

Yiheng Feng
Assistant Professor

Andrew Tarko
Professor

Purdue University

ACKNOWLEDGEMENTS AND DISCLAIMER

Funding for this research was provided by the Center for Connected and Automated Transportation under Grant No. 69A3551747105 of the U.S. Department of Transportation, Office of the Assistant Secretary for Research and Technology (OST-R), University Transportation Centers Program. The contents of this report reflect the views of the authors, who are responsible for the facts and the accuracy of the information presented herein. This document is disseminated under the sponsorship of the U.S. Department of Transportation, University Transportation Centers Program, in the interest of information exchange. The U.S. Government assumes no liability for the contents or use thereof.

Suggested APA Format Citation:

Feng, Y., and Tarko, A. (2023). Development of A Cooperative Perception System, CCAT Report No. 70, The Center for Connected and Automated Transportation, Purdue University, W. Lafayette, IN.

Contacts

For more information

Samuel Labi, Ph.D.
Purdue University
550 Stadium Mall Drive
HAMP G167B
Phone: (765) 494-5926
Email: labi@purdue.edu

CCAT
University of Michigan Transportation Research Institute
2901 Baxter Road
Ann Arbor, MI 48152
uumtri-ccat@umich.edu
(734) 763-2498

Technical Report Documentation Page

1. Report No. CCAT Report No. 70	**2. Government Accession No.**	**3. Recipient's Catalog No.**
4. Title and Subtitle Development of a Cooperative Perception System		**5. Report Date:** August 2023 **6. Performing Organization Code** N/A
7. Author(s) Yiheng Feng, Andrew Tarko		**8. Performing Organization Report No.** N/A
9. Performing Organization Name and Address Center for Connected and Automated Transportation, Purdue University, 550 Stadium Mall Drive, W. Lafayette, IN 47907; and University of Michigan Ann Arbor, 2901 Baxter Rd, Ann Arbor, MI 48109		**10. Work Unit No.** **11. Contract or Grant No.** Contract No. 69A3551747105
12. Sponsoring Agency Name and Address U.S. Department of Transportation Office of the Assistant Secretary for Research and Technology 1200 New Jersey Avenue, SE, Washington, DC 20590		**13. Type of Report & Period Covered:** Final report, April 2022 – August 2023 **14. Sponsoring Agency Code** OST-R
15. Supplementary Notes Conducted under the U.S. DOT Office of the Assistant Secretary for Research and Technology's (OST-R) University Transportation Centers (UTC) program.		
16. Abstract Cooperative perception that integrates sensing capabilities from both infrastructure and vehicles can greatly benefit the transportation system in terms of safety and data acquisition. In this project, a prototype of such a system was developed and evaluated by integrating a Lidar-based infrastructure detection system (facilitated with a portable Traffic Scanner, TScan) with an SAE Level 4 connected and automated vehicle (CAV). Vehicle-to-everything (V2X) communication devices were installed on both the TScan and the CAV to enable real-time message transmission of detection results in the form of SAE J2735 Basic Safety Messages (BSMs). The prototype system was validated using a case study. This aimed at improving CAV situation awareness and protecting vulnerable road user (VRU) safety. The field-testing results demonstrated the benefit of cooperative perception from infrastructure sensors in detecting the occluded VRU and helping the CAV plan safer and smoother trajectories.		
17. Key Words Cooperative Perception; Connected and Automated Vehicles; Roadside Instrumentation; V2X Communication; Intersection Safety; Vulnerable Road Users	**18. Distribution Statement** No restrictions.	

19. Security Classif. (of this report) Unclassified	**20. Security Classif. (of this page)** Unclassified	**21. No. of Pages** 23	**22. Price**
Form DOT F 1700.7 (8-72)	Reproduction of completed page authorized		

TABLE OF CONTENTS

LIST OF FIGURES

CHAPTER 1. INTRODUCTION

Sensing and perception of road traffic and driving environment are critical in autonomous driving and intelligent transportation system (ITS) applications. Camera, radar, and Lidar are commonly used types of sensors in the transportation system for both vehicles and infrastructure. The operational effectiveness of such sensors installed in a vehicle is affected by their limited range and by other vehicles and fixed objects that partially occlude the surroundings of the vehicle. Elevated roadside sensors can effectively reduce the occlusion issue. However, the main downsides of roadside sensors are their detection ability decreasing with distance and their fixed tilting angle are non-optimal for some traffic situations. Nevertheless, adding roadside sensors could significantly enhance the vehicle's perception range and its navigation quality. This requires a cooperative sensing and perception system capable of real-time data transmitting, processing, and fusing information from connected and automated vehicles (CAVs) and roadside sensors. This potential improvement is expected to benefit individual CAVs and flow-level traffic control and analysis in many ITS applications.

Even if some vehicles are connected and capable of receiving and broadcasting traffic and road information, the initial low percentage of such vehicles does not offer both sufficient coverage and rate of information in vehicle-to-vehicle communication. Thus, supplementing the sensing capabilities of CAVs with roadside units is justified. Such a roadside perception system will continue to be beneficial even when the percentage of CAVs is high since the information redundancy improves the resilience and reliability of the system. As already mentioned, the limitation of infrastructure-based sensing systems is that they are installed at fixed locations (e.g., at intersections) and cover a relatively small area (e.g., 100-150m radius). Due to the high cost of infrastructure sensors only a limited number of critical locations (e.g., with complex traffic conditions, higher accident rates) are to be selected for sensor installation. To address the mentioned needs for a cooperative sensing and perception system, we developed and evaluated a prototype of such a system by integrating a portable Lidar-based detection system (i.e., TScan [1-3]) with an SAE Level 4 CAV as shown in Figure 1.

TScan uses Lidar sensors to detect and track in real-time various types of road users, including trucks, cars, pedestrians, and bicycles. The TScan system was initially developed as an instrumented van [1] and then converted to a trailer-based unit [2] for the envisioned end user. TScan's ability of detecting traffic encounters and conflicts was recently evaluated [3] to make it available to road safety management agencies.

The CAV is equipped with a by-wire control system and various onboard sensors including Lidar, camera, and radar. In addition, vehicle-to-everything (V2X) communication devices are installed on both the TScan and the CAV to enable real-time message transmission of perception data including detection results. In this project, we validated the functionality of the cooperative perception system and evaluated its benefit through a case study, which aimed at improving CAV situation awareness and protecting vulnerable road user (VRU) safety. Field testing results showed that the cooperative perception system timely provided the vehicle with advanced information, otherwise not available due to occlusion, which improved both safety and driving comfort.

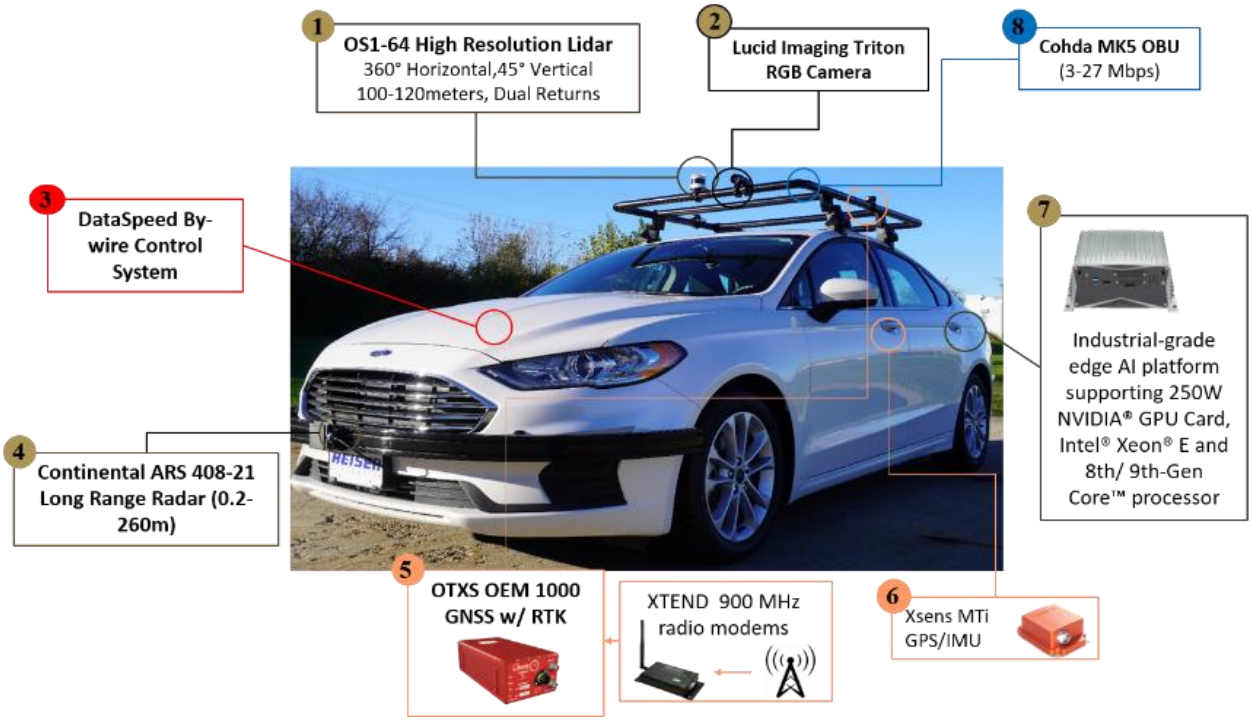

Figure 1 TScan System and Level 4 CAV

CHAPTER 2. SYSTEM DEVELOPMENT

Figure 2 shows the overall structure of the cooperative perception system. In the vehicle platform, a LiDAR sensor is used for perception due to its high-level accuracy in providing depth information and a 360-degree field of view. A clustering-based 3D object detection model from the Autoware[1] autonomous driving platform is used to detect the surrounding objects and the Hungarian algorithm [4] plus Kalman Filter [5] association and tracking model is applied to track the objects and to generate continuous trajectories. The object list generated from the tracking algorithm is fed into the Information Fusion module.

TScan also utilizes LiDARs as perception sensors and applies a similar object detection and tracking pipeline to generate the detected object list. Coordination transformation is performed to convert local coordinates to GPS coordinates. Each object in the list is then encoded into an SAE J2735 Basic Safety Message (BSM) and broadcasted through a roadside unit (RSU). Note that if there are multiple objects in the list, then multiple BSMs are sent at the same time. An onboard unit (OBU) is installed on the vehicle platform to receive the BSMs and to forward the information to the Information Fusion module. The Information Fusion unit uses a predefined area (i.e., the roadway area) to geo-fence the objects and it fuses the object lists by removing redundant observations. The fused information is then input to the Path Planner in which a customized heuristic algorithm provides longitudinal vehicle control while the pure pursuit algorithm [6] provides lateral vehicle control. Finally, the Path Planner outputs the vehicle speed and steering angle to the by-wire control system for execution. In the vehicle platform, all components are synchronized through the robot operating system (ROS). In Figure 2, the light blue boxes highlight the new components in the two systems that enable the cooperative perception function. In the next section, the components of the TScan system and the vehicle platform are described in detail.

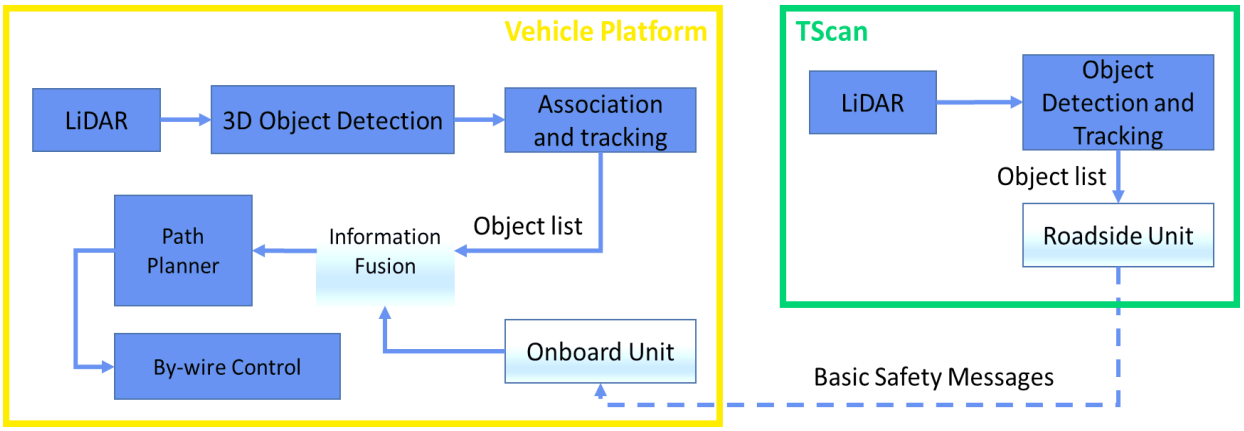

Figure 2 Overall Structure of the Cooperative Perception System

[1] https://github.com/Autoware-AI

1.1 TScan System

Traffic Scanner (TScan) is a portable microscopic traffic data-acquisition system that utilizes LiDAR technology. Two trailer-based prototypes were developed at the Purdue Center for Road Safety with support from the Joint Transportation Research Program (JTRP) of the Indiana Department of Transportation and Purdue University and the NEXTRANS Center at Purdue University [1]. The hardware platform of TScan sensing is shown in Figure 3.

Figure 3 TScan Hardware Platform

TScan consists of two LiDAR units: a Velodyne HDL 32E and an Ouster OS1 64. These sensors are mounted on tilt/pan motors to allow changing the field of view of the system to better cover the area of interest in the field. A fisheye camera is used to record video which is only used for investigating scenes selected by the user. All the processing is based on color blind LiDAR. All the electronics to control the system and a computer to process the data in real time are present in the head unit.

TScan uses a few minutes of data to identify background. Then, during real time operation, the background is removed and the remaining points are clustered. Each cluster potentially represents a moving object. These clusters are tracked over time using a combination of the Kalman filter for state estimation and the Hungarian assignment algorithm for association. The corrected Kalman estimates for every object in the field of view are then broadcast every 0.1 seconds. More details of the TScan system can be found in [1].

1.2 Vehicle Platform

Perception based on 3D point cloud data

In this work, we mainly use LiDAR as the perception sensor. Firstly, we execute a point cloud downsampling process, which aims to downsample the raw point cloud data obtained from the LiDAR sensor on the CAV. The primary goal of downsampling is to eliminate noise from the raw point cloud data, a process influenced by the number of points within a voxel. We have configured the voxel size to be 0.01 meters and the measurement range to be 200 meters.

After downsampling the point cloud, we execute the first stage of ground removal using a ray ground filter from the Autoware platform. In the downsampled point cloud, we initially separate them radially. Then, the ground is identified using geometric information related to the ego vehicle. Within each ray, we determine if a point belongs to the ground based on the distance and angle between points. This method successfully removes the ground that is far away from the ego vehicle, thereby potentially reducing errors in the downstream clustering algorithm. In this study, we set the clipping height at 1 meter and the minimum point distance at 1.5 meters. We divide the point cloud into different rays at intervals of 0.08 radius, and points are checked if their corresponding radius is larger than 0.01. For ray ground filtering, we set the local max slope at 8, the general max slope at 5, and the minimum height threshold at 0.05. Points will be rechecked and reassigned to different classes if their distance to the closest point is greater than 0.2 meters.

After the ground removal, the Euclidean-based clustering method serves as a clustering-based detector for identifying the locations of vehicles and VRUs. Data points that are less than 60 cm above the ground are ignored. This setting is determined by the height of the LiDAR mounted on the CAV to eliminate the impact of stationary road obstacles, such as cement piers, which are near the area of interest of the experiment. In the clustering algorithm, the clustering distance is set to 0.75 meters. The minimum number of points within a cluster is set to 20, and the maximum to 100,000. We also perform another voxelization process to downsample the point cloud and assure the accuracy of the clustering result. At this stage, the leaf size for clustering is set to 0.2 meters. A size-based naïve filtering method is applied to filter out stationary and large objects based on the results from the Euclidean point cloud clustering algorithm. Only clusters of lengths, widths, and heights ranging between 0.1 m and 1 m are recognized as VRUs. The lower bound is incorporated to reduce the impact of noisy predictions.

Association and Tracking Algorithm

After obtaining results from the perception module, the detection results are assigned to trackers and then updated with a Kalman filter. This Kalman filter-based tracking mechanism is inherited from the SORT algorithm [7], which was previously employed for image-based object tracking. Figure 4 illustrates a workflow of how SORT is implemented with real-time perception results from the surrounding environment.

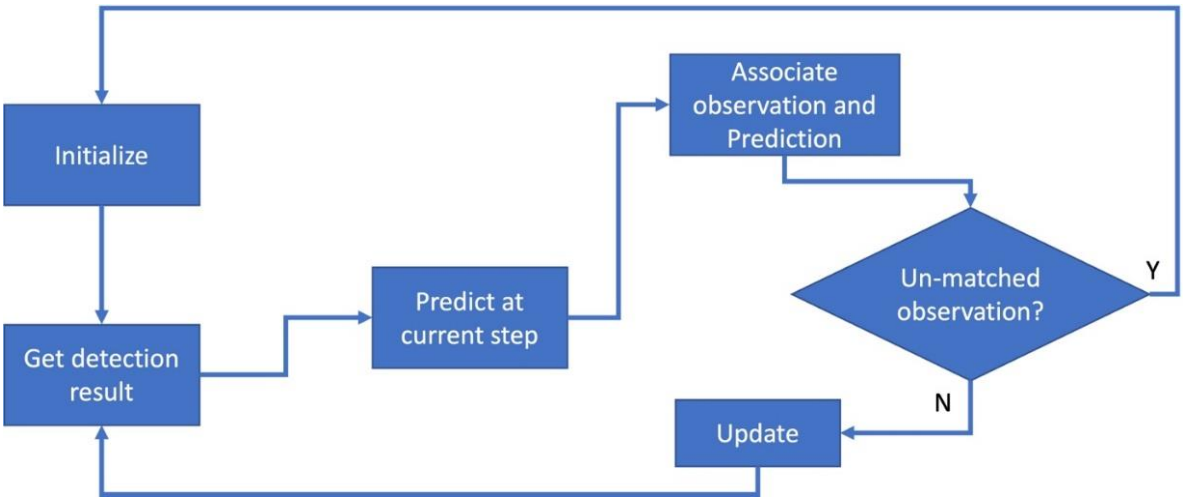

Figure 4 SORT framework with vehicle detection

Detection results, accompanied by corresponding time information, are obtained through the perception module. A constant speed Kalman filter is then applied to predict the expected object location from the previous detection. Subsequently, a cost matrix is calculated based on the prediction and the current observation result. Using the cost matrix, the Hungarian matching algorithm [6] is applied to match the prediction with the current observation. For each initial matching result, the cost is checked to ensure it does not exceed a predefined threshold. If the cost is larger than the threshold, then the prediction for the previous observation is unmatched, and its corresponding track is updated with the prediction only. The unmatched observations are used to initialize new tracks, and each observation is considered as the first frame of each new track. If the prediction from the previous observation is matched with the current observation, the corresponding track is updated with the result of the Kalman filter, which is the posterior result after correction with the matched observation. In this framework, the quality of association relies on the detector and, thus, is sensitive to noise.

Information Fusion

After obtaining data from both the vehicle perception module and BSMs from TScan, we implement decision-level information fusion to reduce redundancy in the downstream path planning module. As implemented in the CARMA system [8], we execute decision-level fusion.

In this work, given the same object, we might have detections from both the CAV and TScan. Multiple detections can impact the performance of the downstream module. Therefore, we first perform a redundancy check, then combine duplicated detections based on location data. If the distance between two detections is less than a certain threshold (e.g., one vehicle length), we consider them to belong to the same vehicle and use the averaged location.

Due to the complexity of the experiment site, there might be objects with similar locations but completely different kinematic profiles. Therefore, the speed of detection results is also taken into consideration when performing decision-level merging. Based on the location, speed, and dimensional information of the detected object, we construct a complete bipartite graph G

= (S, T; E) for decision-level fusion. In this bipartite graph, S represents the set of infrastructure vertices (i.e., bounding boxes detected from the infrastructure side); T represents the set of vehicle vertices (i.e., bounding boxes detected from the vehicle side); and E denotes the set of edges in the graph connecting S and T. Each edge carries a nonnegative cost c(i,j) of objects i and j. This cost function is the weighted sum of multiple factors, including vehicle dynamic features (e.g., location and speed) and appearance features (e.g., the shape of the bounding box). Any edge that carries a cost higher than a predetermined threshold is removed. For the vertices connected to at least one edge, we apply the Kuhn–Munkres algorithm [7] to find the maximum matching between two observations representing a single object. Any unmatched vertices are considered unique observations, which we retain as the results of the cooperative perception process.

In addition to redundancy removal, we conduct geofencing to eliminate all detected objects outside the anticipated detection area. The results, post decision-level fusion from the CAV perception and TScan detection, are then fed into the CAV's path-planning module, which will be introduced in the subsequent section.

Path Planner

The path planner for the CAV can be divided into two parts: lateral control and longitudinal control. Similar to [8], a pure pursuit lateral controller is applied for trajectory following. For longitudinal control of the CAV, the Gipps car-following model [9] is applied to interact with objects in the same lane. Finally, a post encroachment time (PET) [10] based speed planner is implemented when the CAV is interacting with objects from the side (e.g., at an intersection).

For the PET-based speed planner, once an object is detected, we first calculate the potential conflict point location, considering the object's current location, its speed in the x and y directions, and the planned trajectory of the CAV. We then ascertain if the object is close to the conflict point, and a virtual front vehicle (serving as a red signal) will be placed at the conflict point if the object is within a predefined geofencing area, regardless of its speed. In this case, the CAV will yield to the object to avoid the crash. If the object is outside the predefined geofencing area, we calculate the PET for the object and the CAV. If the PET for the object and the CAV is greater than 2 seconds, then the CAV will maintain its constant speed. However, if the PET for the object and CAV is less than two seconds, we determine if the object has already crossed the conflict point. If not, the CAV's speed is reduced to reach the 2 seconds PET (also yield the object). If the object already crossed the conflict point more than 2 seconds ago, then the CAV resumes to the free flow speed.

CHAPTER 3. EXPERIMENTS

3.1 TScan Detection Accuracy Test

First, we validated the accuracy of the TScan detection results. It is critical that the TScan sends accurate information regarding object locations. The experiment was conducted in the North Stadium parking lot on Purdue University campus on March 17, 2023. The TScan system was staged at the north end of the parking lot while the CAV was circling the parking lot as shown in Figure 5(a). The blue block represented the TScan system. The yellow shaded areas represented the geo-fencing area of TScan and the red circle approximated CAV's driving route. Detection results from the TScan (i.e., the CAV) were sent through BSM to the CAV. The location data in the BSM (i.e., GPS coordinates) were compared with the GPS coordinates collected from the CAV's RTK GPS. We considered the coordinates collected from the RTK GPS as ground truth, since it has centimeter-level accuracy.

The distribution of the detection error is shown in Figure 5(b). The coordinates are defined to be consistent with the vehicle coordinate system, where the X-axis points forward from the vehicle and the Y-axis point to the left when facing forward. Most of the errors in the Y-axis ranged from -1.5m to 0.5m with a few outliners between -2.5m to -3m. There was a systematic error in the X-axis since all errors were positive ranging from about 0.5m to 2.5m. However, TScan considered the center of the bounding box as its coordinate while the RTK GPS receiver was not installed in the middle of the vehicle. The distance from the GPS receiver to the center of the vehicle along the X-axis is about 1.60m. As a result, the actual error distribution along the X-axis is about -0.9m to 0.9m. Since the distance from the GPS receiver to the center of the vehicle along the Y-axis is only 0.09m, we ignored this small difference. In summary, the error distribution validated the detection accuracy of the TScan system.

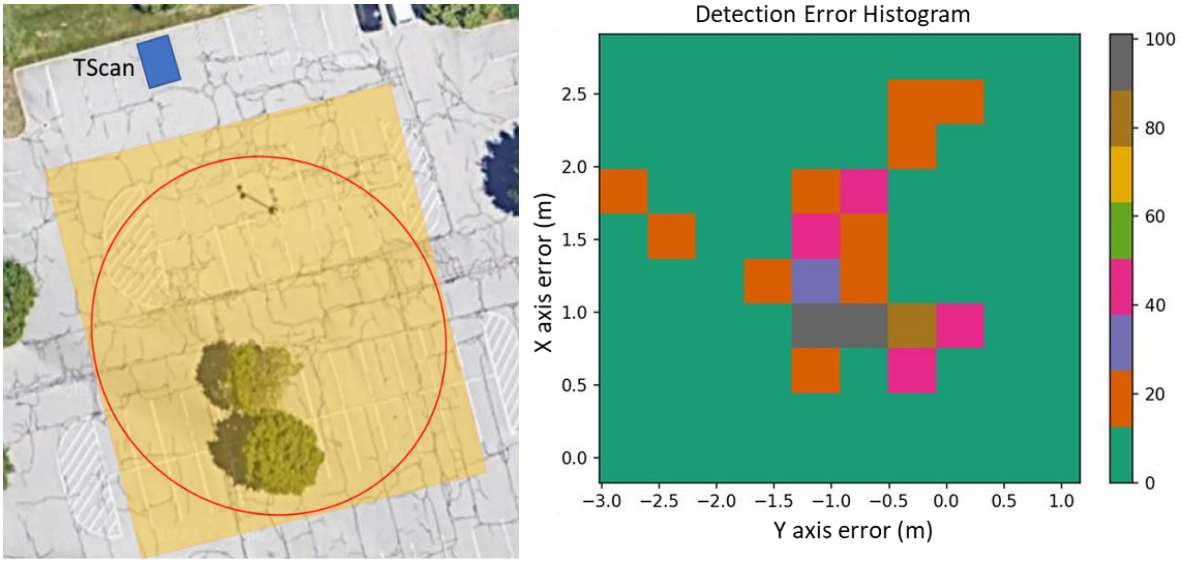

(a) Test setup (b) Error distribution

Figure 5 TScan Detection Error Analysis

3.2 Case Study

Scenario Setup

We designed a case study to demonstrate the benefit of the cooperative perception system in improving VRU safety at intersections. The experiment was staged at the Purdue Research Park parking lot as shown in Figure 6 (a). In the experiment design, a VRU was traveling from west to east (red route) while the CAV was traveling from south to north (green route). Their routes have a conflict point at the T-intersection. Due to the building and parked vehicles (blue blocks), the VRU was occluded and can't be observed by the onboard sensors of the CAV when it was approaching the T-intersection. TScan (yellow circle) was located at the northeast corner of the intersection so that it can observe the VRU and CAV at the same time. The orange-shaded areas represented TScan's geo-fencing areas. To ensure safe tests, we built the "VRU" with a Backfire G2 skateboard attached to two large U-Hual boxes. The size of the "VRU" was similar to a teenager (about 50 inches tall) and we named him "Jack". The skateboard can be controlled by a remote with different speeds. We conducted three different experiments described as follows.

- Experiment 1: The VRU and the vehicle are approaching the intersection at the same time **without** TScan and the vehicle is driven by **a human driver**.
- Experiment 2: The VRU and the vehicle are approaching the intersection at the same time **without** TScan and the vehicle is driven **autonomously**.
- Experiment 3: The VRU and the vehicle are approaching the intersection at the same time **with** TScan and the vehicle is driven **autonomously**.

In Experiments 2 and 3, the free flow speed of the CAV was set to 5 m/s. In Experiment 1, the driver was asked to drive at a similar speed of 10mph. Our central hypothesis was that TScan was able to detect the VRU before he arrived at the intersection which led to a safer and smoother vehicle reaction.

(a) Scenario Demonstration (b) VRU "Reckless Jack"

Figure 6 Case Study Scenario Design

CHAPTER 4. FINDINGS

In the first experiment, a human driver (from our research team) was asked to drive the vehicle to pass the intersection without knowing the VRU's existence. The driver didn't even notice the appearance of the VRU from the left and crashed into the object as shown in Figure 7 (a). The speed profile of the vehicle observed from the TScan is shown in Figure 7(b). It can be seen that at the time of impact, the driver didn't take any actions (e.g., brake).

(a) Impact time point of the vehicle and VRU

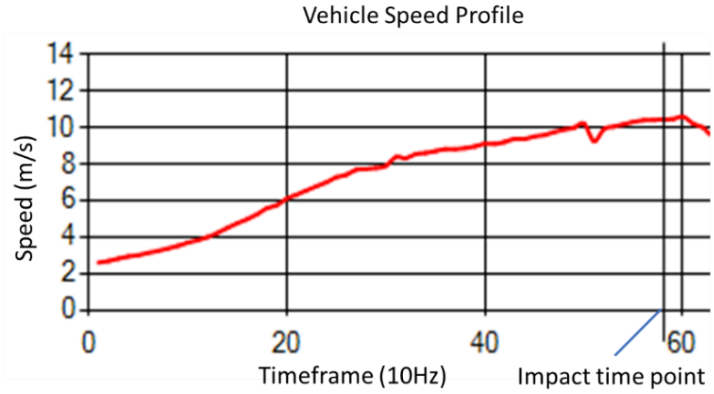

(b) Vehicle speed profile

Figure 7 Results of Experiment 1

In the second experiment, the autonomous driving system took control of the vehicle and followed the same route, and interacted with the VRU. Figure 8 (a) shows the snapshot of the first time point that the VRU was detected from the LiDAR (the white box). The distance to the CAV was only 14.0m. Figure 8 (b) shows the front camera view at the same moment. It can be seen that when the LiDAR captured the VRU, he was already very close to the intersection. The CAV detected a potential conflict and applied a hard break to avoid the crash. The trajectory and speed profiles of the CAV and the VRU (after detection) are shown in Figure 9. The three time points in the trajectory plot are the first time point the VRU was detected (31.7s), the time point the VRU passed the conflict point (33.0s), and the time point the CAV passed the conflict point (38.1s). From the CAV's speed profile, it can be seen that after the detection of the VRU at 31.7s, it applied a hard brake with an average deceleration of -1.32 m/s^2 and a maximum deceleration of -5.12 m/s^2 to avoid the crash. Compared to Experiment 1 with human drivers, the vehicle was able to make a complete stop and avoid the crash due to the detection of VRU and shorter reaction time.

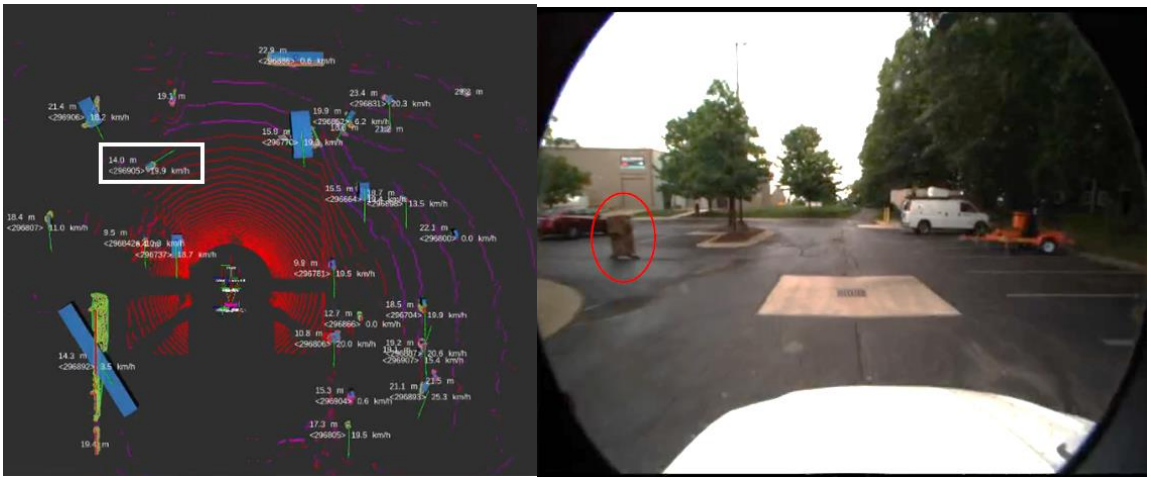

(a) Lidar detection results (b) Camera View

Figure 8 Experiment 2: Lidar and Camera View

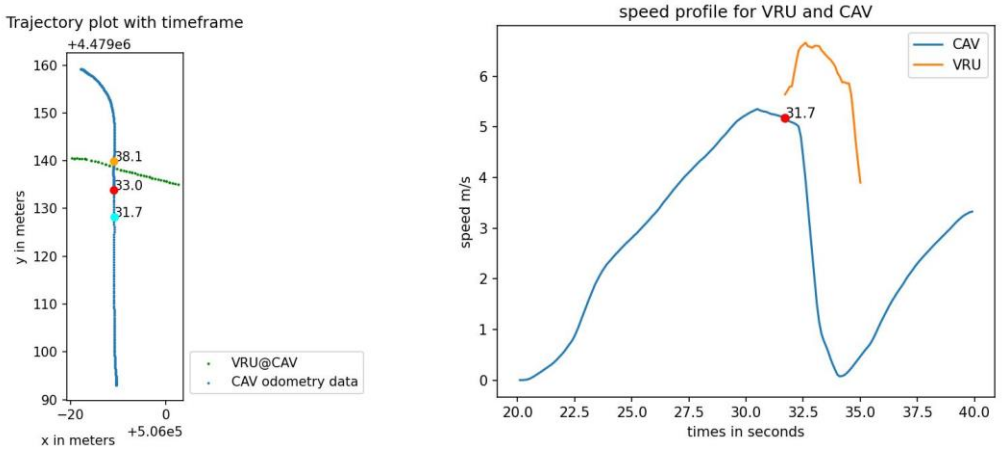

(a) Trajectory profiles (b) Speed profiles

Figure 9 CAV and VRU trajectory and speed profiles of experiment 2

In the third experiment, the CAV and VRU were approaching the intersection the same way as in Experiment 2. In this experiment, TScan detected the objects in the geofenced area and broadcast detected objects in real-time to the vehicle through BSMs. Figure 10 shows a few snapshots from the TScan fisheye camera recording of the whole scenario.

(a) Objects near the intersection @5:20s

(b) Objects started interaction @5:23s

(c) CAV stopped for VRU @5:26s

(d) CAV passed conflict point @5:30s

Figure 10 Experiment 3 Scenario Demonstration

The trajectory and speed profiles of the CAV and the VRU collected from the vehicle platform are shown in Figure 11. The four time points in the trajectory plot are the first time point the VRU's information was received by the CAV from TScan (15.95s), the time point the CAV started to react to the VRU due to planned PET (16.69s), the time point the VRU passed the conflict point (21.74s), and the time point the CAV passed the conflict point (27.43s). The speed profile of CAV showed a smoother trend with an average deceleration of -0.49 m/s^2 and a maximum deceleration of -2.21 m/s^2, which was much lower than those in Experiment 2.

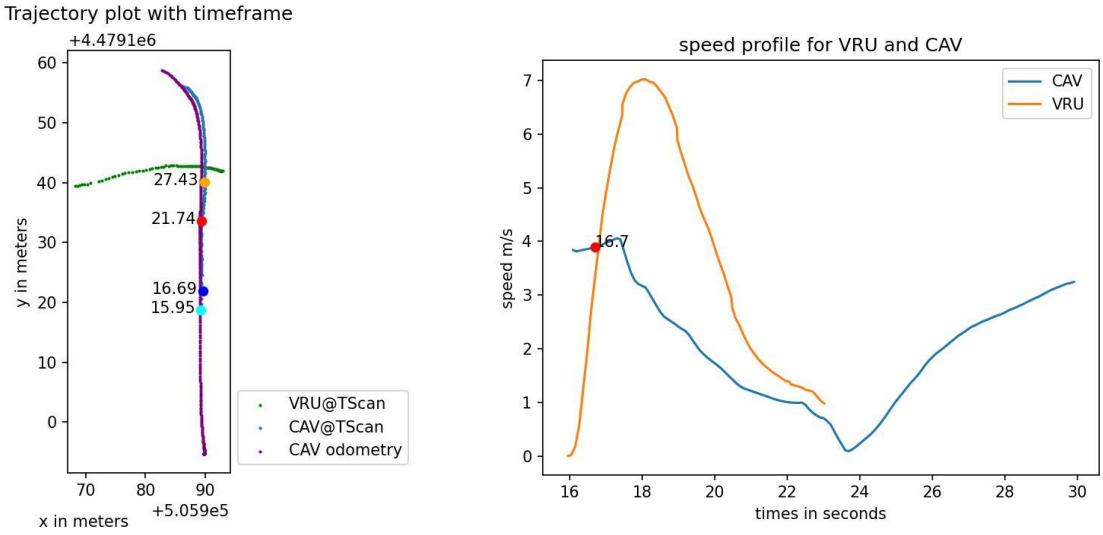

(a) Trajectory profiles (b) Speed profiles

Figure 11 CAV and VRU trajectory and speed profiles of experiment 3 (from CAV)

Figure 12 shows the corresponding trajectory and speed profiles recorded from the TScan system of the same experiment. The speed profile of CAV also shows that it has slowed down to allow the VRU to pass through. The thin yellow line shows the predicted future trajectory of the detected objects. The dotted yellow shows the past trajectory.

This experiment demonstrated the benefit of cooperative perception from infrastructure sensors in improving CAV situation awareness, safety, and driving comfort as well as VRU safety. The safety impact can be further demonstrated by the PET plots between the CAV and VRU in Figure 13. Figure 13 (a) shows the PET profile in Experiment 2 from the first detection of the VRU until the VRU passed the conflict point. When the VRU was detected, the PET was already very low. Even though the vehicle took a hard brake, the final PET when the VRU passing the conflict point was still smaller than 1s. Figure 13 (b) shows the PET profile in Experiment 3 from the time point that the TScan detected the VRU until the VRU passed the conflict point. It can be seen that the PET dropped from 5s to around 1s when the CAV started to react to the VRU (at 16.69s). Afterward, the PET started to increase and maintained within a safe boundary.

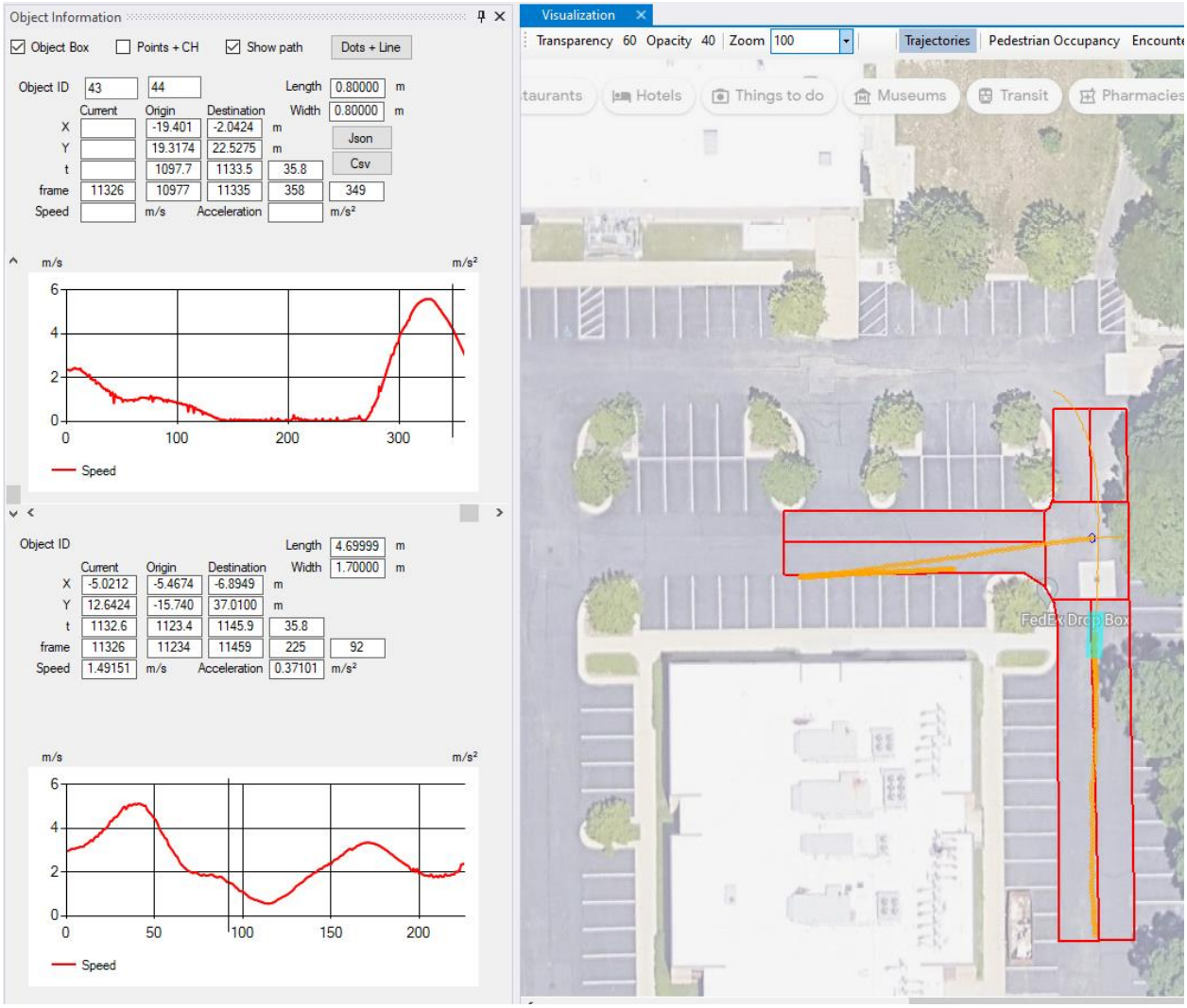

Figure 12 CAV and VRU trajectory and speed profiles of experiment 3 (from TScan)

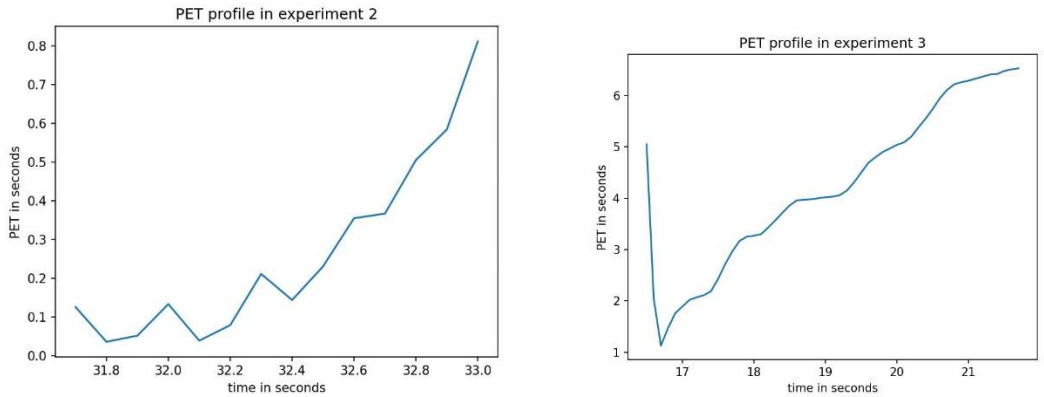

(a) PET profile in experiment 2

(b) PET profile in experiment 3

Figure 13 PET Profile Comparison

CHAPTER 5. RECOMMENDATIONS

5.1. Introduction

Although in this project, we mainly utilized the cooperative perception system for CAV path planning and VRU protection, such systems can be implemented in many other applications. For example, detections from both infrastructure and CAV sensors can be fused to improve data collection and augment the penetration rate for real time traffic management such as intersection management [13,14] and eco-routing [15,16]. Meanwhile, the offline processed trajectories can be further utilized to investigate long-term safety performance such as traffic conflicts and crash estimation [17,18].

CHAPTER 6. OUTPUTS, OUTCOMES, AND IMPACTS

The developed cooperative perception system has great benefits in improving safety for connected and automated vehicles by improved sensing and perception, especially under occluded and long-range situations. Meanwhile, different from most existing infrastructure-based sensing systems, the TScan system is portable and can be relocated to different locations as the environments and traffic conditions change. This feature brings great flexibility and adaptation over fixed-location perception systems. The proposed system has the potential to be implemented at real-world intersections in the near future.

The following outputs were generated during the performance of this project:

Conference Proceeding:

Chen, H., Bandaru V.K., Wang, Y., Romero, M.A., Tarko A., and Feng, Y. (2023). A Cooperative Perception System for Aiding CAVs Navigation and Improving Safety, Accepted in the Proceedings of the 2024 TRB Annual Meeting, Washington, DC. The paper has also been recommended for publication in Transportation Research Record in 2024.

The research project supported two graduate students (Yilin Wang, Vamsi Bandaru) and a postdoc (Hanlin Chen). Materials from the project helped support a graduate level course – CE 565 (Traffic operations and controls).

A video of the project was published online and can be accessed at:
https://www.youtube.com/watch?v=5i9v8Sgasb8

REFERENCES

[1]Tarko, A. P., Ariyur, K. B., Romero, M. A., Bandaru, V. K., & Lizarazo, C. G. (2016). TScan: Stationary LiDAR for traffic and safety studies—Object detection and tracking (Joint Transportation Research Program Publication No. FHWA/IN/ JTRP-2016/24). West Lafayette, IN: Purdue University. http://dx.doi.org/10.5703/128828431634

[2] Bandaru V. K., Romero M. A., Lizarazo C., Tarko A. P. TScan – Stationary LiDAR for Traffic and Safety Applications: Vehicle Interpretation and Tracking. Joint Transportation Research Program Publication No. FHWA/IN/JTRP-2021/31. Purdue University, West Lafayette, IN, 2021

[3]Tarko, A. P., Romero, M. A., Bandaru, V. K., & Shi, X. (2023). Guidelines for evaluating safety using traffic encounters: Proactive crash estimation on roadways with conventional and autonomous vehicle scenarios (Joint Transportation Research Program Publication No. FHWA/IN/JTRP-2023/02). West Lafayette, IN: Purdue University. https://doi. org/10.5703/128828431758

[2] Kuhn, H. W. (1955). The Hungarian method for the assignment problem. Naval research logistics quarterly, 2(1-2), 83-97.

[3] Welch, G., & Bishop, G. (1995). An introduction to the Kalman filter.

[4] Coulter, R. C. (1992). Implementation of the pure pursuit path tracking algorithm (pp. 92-01). Carnegie Mellon University, The Robotics Institute.

[5] Bewley, A., Ge, Z., Ott, L., Ramos, F., & Upcroft, B. (2016, September). Simple online and real-time tracking. In 2016 IEEE international conference on image processing (ICIP) (pp. 3464-3468). IEEE.

[6] Chen, H., Liu, B., Zhang, X., Qian, F., Mao, Z. M., & Feng, Y. (2022). A Cooperative Perception Environment for Traffic Operations and Control. arXiv preprint arXiv:2208.02792.

[7] Zhu, H., Liu, D., Zhang, S., Zhu, Y., Teng, L., & Teng, S. (2016). Solving the many to many assignment problem by improving the Kuhn–Munkres algorithm with backtracking. Theoretical Computer Science, 618, 30-41.

[8] Chen, H., Luo, R., & Feng, Y. (2023). Improving Autonomous Vehicle Mapping and Navigation in Work Zones Using Crowdsourcing Vehicle Trajectories. arXiv preprint arXiv:2301.09194.

[9] Gipps, P. G. (1981). A behavioural car-following model for computer simulation. Transportation research part B: methodological, 15(2), 105-111.

[10] Gettman, D., & Head, L. (2003). Surrogate safety measures from traffic simulation models. Transportation Research Record, 1840(1), 104-115.

[11] Feng, Y., Head, K. L., Khoshmagham, S., & Zamanipour, M. (2015). A real-time adaptive signal control in a connected vehicle environment. Transportation Research Part C: Emerging Technologies, 55, 460-473.

[12] Yang, Z., Feng, Y., & Liu, H. X. (2021). A cooperative driving framework for urban arterials in mixed traffic conditions. Transportation research part C: emerging technologies, 124, 102918.

[13] Djavadian, S., R. Tu, B. Farooq, and M. Hatzopoulou. Multi-Objective Eco-Routing for Dynamic Control of Connected & Automated Vehicles. Transportation Research Part D: Transport and Environment, Vol. 87, 2020, p. 102513.https://doi.org/10.1016/j.trd.2020.102513.

[14] Zeng, W., T. Miwa, and T. Morikawa. Eco-Routing Problem Considering Fuel Consumption and Probabilistic Travel Time Budget. Transportation Research Part D: Transport and Environment, Vol. 78, 2020, p. 102219. https://doi.org/10.1016/j.trd.2019.102219.

[15] Tarko, A. P. (2021). A unifying view on traffic conflicts and their connection with crashes. Accident Analysis & Prevention, 158, 106187.

[16] Tarko, A. (2019). Measuring road safety with surrogate events. Elsevier.